1.2 THE BOWEN RATIO OVER SEA ICE

Edgar L Andreas*
NorthWest Research Associates, Inc.; Lebanon, New Hampshire

and

Rachel E. Jordan
Jordan Environmental Modeling, PC; Hanover, New Hampshire

1. INTRODUCTION

The Bowen ratio,

$$\mathrm{Bo} \equiv H_s / H_L \ , \qquad (1.1)$$

occurs repeatedly throughout micrometeorology (e.g., Panofsky and Dutton 1984; Garratt 1992; Lewis 1995). In (1.1), H_s is the turbulent surface flux of sensible heat, and H_L is the turbulent surface flux of latent heat.

A common use for the Bowen ratio is in the so-called Bowen ratio and energy budget method (Fleagle and Businger 1980, p. 290f.; Brutsaert 1982, p. 210; Arya 1988, p. 191; Stull 1988, p. 430). Other uses are in interpreting sonic anemometer data (e.g., Schotanus et al. 1983) and in specifying the Obukhov length, the stratification parameter in the atmospheric surface layer, when the latent heat flux is unknown (e.g., Busch 1973; Andreas 1992). Wesley (1976) and Andreas (1988) showed how electromagnetic propagation in the surface layer is sensitive to the Bowen ratio.

In a bulk flux algorithm, the turbulent surface heat fluxes are parameterized as (e.g., Fairall et al. 1996; Andreas et al. 2010a, 2010b)

$$H_s = \rho c_p C_{Hr} S_r (\Theta_s - \Theta_r) \ , \qquad (1.2a)$$

$$H_L = \rho L_v C_{Er} S_r (Q_s - Q_r) \ . \qquad (1.2b)$$

Here, ρ is the air density; c_p, the specific heat of air at constant pressure; L_v, the latent heat of vaporization or sublimation; S_r, the effective wind speed at reference height r; Θ_r and Q_r, the potential temperature and specific humidity at height r; and Θ_s and Q_s, the potential temperature and specific humidity at the surface. Finally, C_{Hr} and C_{Er} are the transfer coefficients for sensible and latent heat, respectively, appropriate for height r. In our convention, H_s and H_L are positive when the flux is from surface to air.

From (1.1) and (1.2), we see that the Bowen ratio can also be expressed as

$$\mathrm{Bo} = \frac{c_p C_{Hr} (\Theta_s - \Theta_r)}{L_v C_{Er} (Q_s - Q_r)} \ . \qquad (1.3)$$

Thus, if we know the gradients $\Theta_s - \Theta_r$ and $Q_s - Q_r$ and have measured either H_s or H_L directly, we can calculate the other flux by knowing the Bowen ratio. Notice also that the signs of $\Theta_s - \Theta_r$ and $Q_s - Q_r$ dictate the signs of H_s, H_L, and Bo.

Over saturated surfaces, where we can assume that Q_s in (1.2) and (1.3) can be calculated as the saturation humidity at temperature Θ_s, the Bowen ratio is tightly constrained. Typical saturated surfaces include the open ocean, sea ice, large lakes, extensive snow fields, and large glaciers.

Philip (1987) theoretically established this constraint on the Bowen ratio for the case $H_s > 0$ and $H_L > 0$ under the assumption that the near-surface humidity was not above its saturation value (i.e., no fog). Andreas (1989; see also Philip 1989) extended Philip's ideas to also formulate constraints for the cases $H_s < 0$, $H_L > 0$ and $H_s < 0$, $H_L < 0$. Andreas and Cash (1996) subsequently evaluated all three of these constraints using data collected over the open ocean, over sea ice, over large lakes, and over snow-covered ground.

As an example of the value of this approach, Jo et al. (2002) used it to publish a climatology of the Bowen ratio for the world ocean. Their implied objective was to provide a way to estimate both H_s and H_L over the ocean from satellite remote sensing.

Here, we repeat some of the analyses in Andreas and Cash (1996) but focus exclusively on the Bowen ratio over sea ice. We have two large

* *Corresponding author address:* Dr. Edgar L Andreas, NorthWest Research Associates, Inc. (Seattle Division), 25 Eagle Ridge, Lebanon, NH 03766-1900; e-mail: eandreas@nwra.com.

data sets for these analyses: from Ice Station Weddell and from SHEBA, the year-long experiment on the Surface Heat Budget of the Arctic Ocean. As with Jo et al. (2002), one potential application for our analysis is to infer the turbulent heat flux terms in the surface energy budget over sea ice from satellites.

2. CONTRAINTS ON THE BOWEN RATIO

Yet another way to formulate the sensible and latent heat fluxes in the atmospheric surface layer is with the turbulent diffusivities for temperature and humidity, K_θ and K_q, respectively (cf. Dyer 1974; Philip 1987):

$$H_s = -\rho c_p K_\theta(z)\partial\Theta/\partial z \ , \qquad (2.1a)$$

$$H_L = -\rho L_v K_q(z)\partial Q/\partial z \ , \qquad (2.1b)$$

where z is the height. Because there is no compelling evidence that K_θ and K_q are different (e.g., Högström 1996), (2.1) reduces to

$$\frac{H_s}{H_L} = \mathrm{Bo} = \frac{c_p}{L_v \partial Q/\partial\Theta} \ . \qquad (2.2)$$

Since H_s and H_L are constants with height in the atmospheric surface layer over a horizontally homogeneous surface, $\partial Q/\partial\Theta$ must be also. We can thus evaluate it at the surface, which has temperature Θ_s. (The physical surface temperature and the potential temperature Θ_s are commonly taken to be the same over surfaces like snow, sea ice, and the open ocean.) Moreover, if the surface is saturated, $\partial Q/\partial\Theta\big|_{\Theta_s}$ is the relation for the saturation specific humidity. Hence, following Philip (1987), we define

$$\mathrm{Bo}_* \equiv \left.\frac{c_p}{L_v \partial Q_{sat}/\partial\Theta}\right|_{\Theta_s} \ . \qquad (2.3)$$

Andreas and Cash (1996) give the equations that we use for calculating this quantity.

Figure 1 shows that Bo_* is a strong function of temperature because the saturation vapor pressure—used in calculating $\partial Q_{sat}/\partial\Theta\big|_{\Theta_s}$—is an exponentially increasing function of temperature. Priestley and Taylor (1972) and Hicks and Hess (1977) used Bo_* to estimate the Bowen ratio and to predict evaporation over saturated surfaces.

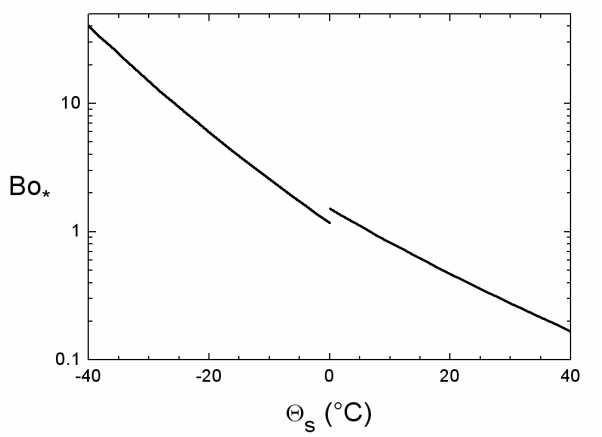

FIG.1. Bo_* from (2.3) as a function of surface temperature, Θ_s. For these calculations, the barometric pressure was 1000 mb and the surface salinity was zero. The discontinuity at $\Theta_s = 0$°C occurs because the calculation switches from using the saturation vapor pressure over ice and the latent heat of sublimation for L_v for temperatures less than 0°C to using saturation over water and the latent heat of evaporation for temperatures above 0°C.

Raupach (2001) formulated a theory of equilibrium evaporation in terms of Bo_*.

On assuming, for the case when $H_s > 0$ and $H_L > 0$, that the humidity above a saturated surface is not above its saturation value, Philip (1987) deduced

$$\frac{\partial Q}{\partial\Theta} \geq \left.\frac{\partial Q_{sat}}{\partial\Theta}\right|_{\Theta_s} \ . \qquad (2.4)$$

Consequently, in this case, from (2.2)–(2.4),

$$\mathrm{Bo} \leq \mathrm{Bo}_* \ . \qquad (2.5)$$

Panel a in Fig. 2 graphically demonstrates this argument. The heavy curved line is $Q_{sat}(\Theta)$. At Θ_s, the straight line tangent to the curve is $\partial Q_{sat}/\partial\Theta\big|_{\Theta_s}$. For $H_s > 0$ and $H_L > 0$, the air temperature and specific humidity must be in the sector indicated by the shading. Thus, $\partial Q/\partial\Theta \geq \partial Q_{sat}/\partial\Theta\big|_{\Theta_s}$ and $\mathrm{Bo} \leq \mathrm{Bo}_*$.

But besides being positive, both H_s and H_L can conceivably be negative or zero. Thus, there are nine combinations of H_s and H_L. Figure 2 depicts all of these combinations and highlights their implication for constraints on the Bowen ratio.

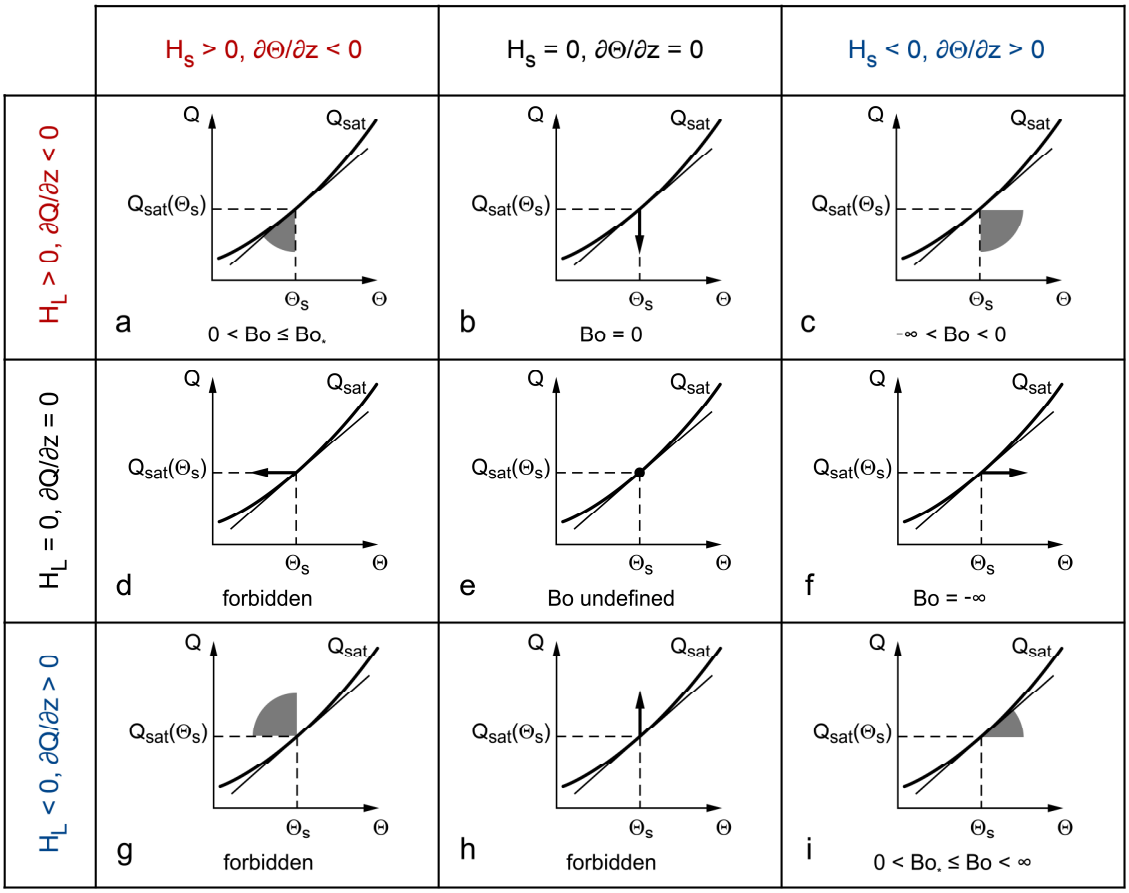

FIG 2. Nine combinations of sensible (H_s) and latent (H_L) heat fluxes and what they say about the Bowen ratio (Bo). The flux is assumed to be down the respective gradient: $\partial\Theta/\partial z$ for sensible heat, and $\partial Q/\partial z$ for latent heat. In each panel, the thicker, curved line is $Q_{sat}(\Theta)$, the relation for saturation in specific humidity. Θ_s is the surface temperature. The thin, straight line tangent to the Q_{sat} curve at Θ_s is $\partial Q_{sat}/\partial\Theta\big|_{\Theta_s}$ and is used in defining Bo_*, (2.3). The shaded areas show where the Q and Θ values above the surface must lie for the given gradients. Heavy arrows indicate that Q or Θ must lie along these lines. The dot in panel e shows the only values that Q and Θ can assume. Any values of Q and Θ that lie above the $Q_{sat}(\Theta)$ line are forbidden by our assumption that the near-surface air is not super-saturated.

Some combinations are forbidden under the assumption of a saturated surface but no super-saturation above the surface: namely, the cases in panels d, g, and h. The cases $H_s = 0$, $H_L > 0$ (panel b) and $H_s < 0$, $H_L = 0$ (panel f) are trivial because Bo = 0 for the former and Bo = –∞ for the latter. In the case $H_s = 0$, $H_L = 0$ (panel e), Bo is undefined.

Using arguments as above for the case $H_s > 0$, $H_L > 0$, Andreas (1989) showed that the case $H_s < 0$, $H_L < 0$ (panel i) also is constrained by Bo_*. But now the constraint (2.4) becomes

$$\frac{\partial Q}{\partial \Theta} \leq \left.\frac{\partial Q_{sat}}{\partial \Theta}\right|_{\Theta_s} . \qquad (2.6)$$

As a result, when $H_s < 0$ and $H_L < 0$,

$$Bo \geq Bo_* . \qquad (2.7)$$

Finally, Andreas and Cash (1996) suggested that, for the case $H_s < 0$, $H_L > 0$ (panel c),

$$Bo \approx -Bo_* . \qquad (2.8)$$

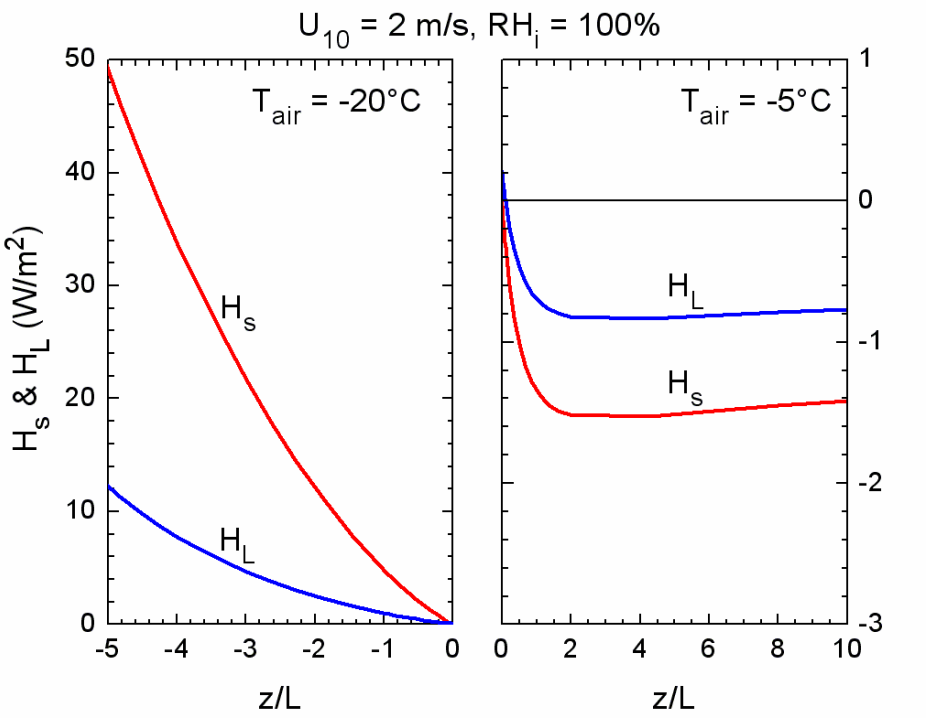

FIG. 3. Sensible and latent heat fluxes as a function of surface layer stratification, z/L, predicted by the winter sea ice algorithm of Andreas et al. (2010b). In all cases, the 10-m wind speed was 2 m s^{-1}, the 10-m relative humidity with respect to ice saturation was 100% (Andreas et al. 2002), and the barometric pressure was 1000 mb. In the unstable panel ($z/L < 0$), the 10-m air temperature was fixed at –20°C, and the surface temperature was incrementally raised from –20°C to produce increasing instability. In the stable panel ($z/L > 0$), the 10-m air temperature was fixed at –5°C, and the surface temperature was lowered from –5°C to produce increasing stability.

Over the saturated surfaces that they studied, Andreas and Cash (1996) found that three regimes in Fig. 2 dominate: the cases $H_s > 0$, $H_L > 0$; $H_s < 0$, $H_L < 0$; and $H_s < 0$, $H_L > 0$ (panels a, i, and c). Over 90% of the measured fluxes that they analyzed fell into one of these combinations.

Figure 3 shows how these three flux combinations occur over sea ice. Here, we used the flux algorithm that Andreas et al. (2010b) developed to estimate sensible and latent heat fluxes over winter sea ice for a wide range in atmospheric stratification, z/L, where L is the Obukhov length and z is the reference height r in (1.2). In unstable stratification, $H_s > 0$ and $H_L > 0$. In weakly stable stratification, $H_s < 0$ and $H_L > 0$. But in stronger stable stratification, both fluxes are downward: $H_s < 0$ and $H_L < 0$. Our flux algorithm predicted no other combinations.

Andreas and Cash (1996) found that the constraints (2.5), (2.7), and (2.8) were useful in quantifying the Bowen ratio in these three dominant flux regimes. We repeat some of their analyses here using data from SHEBA and Ice Station Weddell.

3. DATA

Other sources have already described the SHEBA and Ice Station Weddell data in detail (e.g., Persson et al. 2002; Andreas et al. 2002, 2004, 2005, 2010a, 2010b). Briefly, SHEBA featured the main Atmospheric Surface Flux Group 20-m tower and 3–4 remote sites instrumented with Flux-PAM (portable automated mesonet) stations from the NCAR instrument pool (Militzer et al. 1995).

The main tower measured the sensible heat flux (H_s) with sonic anemometer/thermometers, the potential temperature (Θ), and the specific humidity (Q) hourly at five levels. We use the median of each of these five values in our analysis. The tower also measured the latent heat

TABLE 1. Data used here come from Ice Station Weddell (ISW) and from four SHEBA sites: the SHEBA Atmospheric Surface Flux Group tower, and three Flux-PAM sites (Atlanta, Baltimore, and Florida). We consider two types of data: direct eddy-covariance measurements of the sensible (H_s) and latent (H_L) heat fluxes, and the signs of H_s and H_L implied by the signs of the measured surface-air potential temperature ($\Delta\Theta = \Theta_s - \Theta_r$) and specific humidity ($\Delta Q = Q_s - Q_r$) differences. The "Number of Observations" tallies the hours of useful data from each source. The three columns of flux regimes show the percentage of the observations in each regime. The right column reports the percentage total of these three regimes.

Source	Number of Observations	$H_s > 0$ $H_L > 0$ (%)	$H_s < 0$ $H_L < 0$ (%)	$H_s < 0$ $H_L > 0$ (%)	Total, these three cases (%)
From eddy-covariance measurements					
SHEBA Tower	2859	36.4	31.0	25.8	93.2
ISW	1031	31.6	43.6	15.3	90.5
From measurements of $\Delta\Theta$ and ΔQ					
SHEBA Tower	7447	28.2	53.6	16.4	98.2
SHEBA Atlanta	5098	22.7	52.6	21.3	96.6
SHEBA Baltimore	4473	22.9	57.2	10.7	90.8
SHEBA Florida	5541	19.8	59.6	14.1	93.5
ISW	1782	8.1	80.3	9.3	97.7

flux (H_L) at one level with an Ophir hygrometer in combination with a nearby sonic. We obtained the surface temperature (Θ_s) near the tower from up-looking and down-looking broadband longwave radiometers.

Here, we also use data from the SHEBA Flux-PAM sites named Atlanta, Baltimore, and Florida since each of these had nearly year-long records of hourly data. Although each of these sites measured H_s with a sonic anemometer/thermometer, they did not make a corresponding measurement of H_L. Hence, we use only the $\Theta_s - \Theta_r$ and $Q_s - Q_r$ values from these. Each PAM station measured Θ_r and Q_r at one height. As with the tower data, we inferred Θ_s and Q_s for these sites from the up-looking and down-looking longwave radiometers.

On Ice Station Weddell, we measured H_s and H_L at one height with a sonic anemometer/thermometer and a Lyman-alpha hygrometer. We measured the air temperature and the dew point at the same height with a platinum resistance thermometer and a cooled-mirror dew-point hygrometer, respectively. The surface temperature came from a Barnes PRT-5 precision radiation thermometer; we corrected this measurement for the reflected incoming longwave radiation.

We have approximately 11 months of data from each of the SHEBA sites and about 95 days of data from Ice Station Weddell. All data are hourly averages.

4. FLUX REGIMES

To demonstrate the conceptual utility of Fig. 2, we sorted the SHEBA and Ice Station Weddell data into flux regimes in Table 1. We have two types of data. The main SHEBA tower and Ice Station Weddell measured both H_s and H_L with eddy-covariance sensors. These results are the first two lines in Table 1. From the SHEBA tower, Ice Station Weddell, and the three SHEBA Flux-PAM sites (Atlanta, Baltimore, and Florida), we could also infer the signs of H_s and H_L from independent measurements of $\Delta\Theta \equiv \Theta_s - \Theta_r$ and

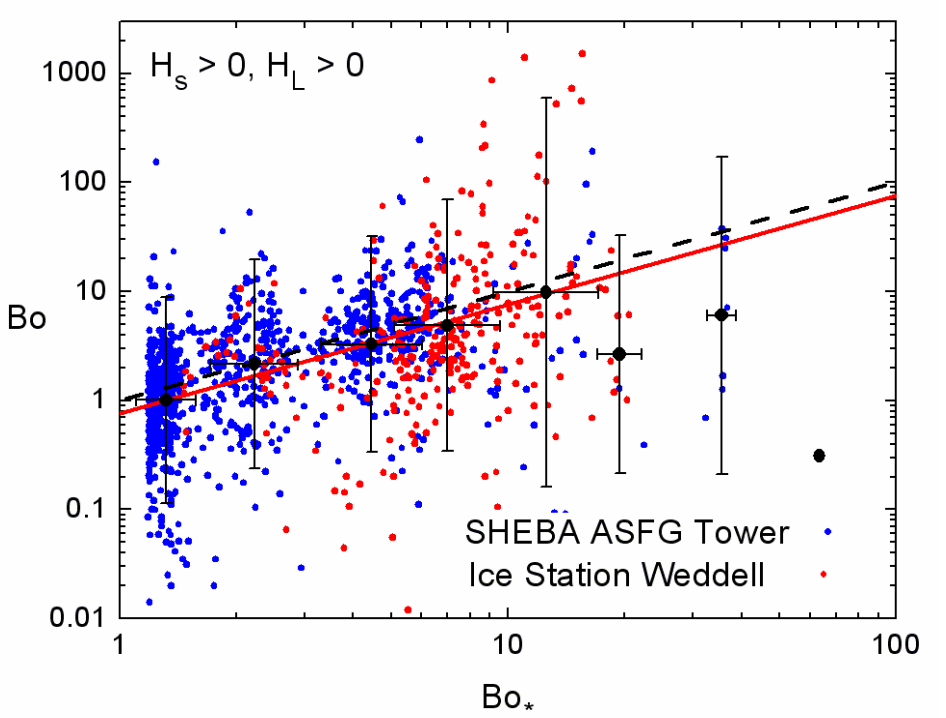

FIG 4. Values of the Bowen ratio calculated from values of H_s and H_L measured hourly on the SHEBA Atmospheric Surface Flux Group tower and on Ice Station Weddell are compared with corresponding values of Bo_* computed from (2.3). The plot is for cases when $H_s > 0$ and $H_L > 0$. The black circles are averages in Bo_* bins, where there are four bins per decade. The error bars are ±2 standard deviations. The black dashed line is 1:1; the red line is the best fit for which the power of Bo_* is one, (5.1).

$\Delta Q \equiv Q_s - Q_r$ [see (1.2)]. These results are in the bottom five lines in Table 1.

In each of the seven datasets, the three flux regimes $H_s > 0$, $H_L > 0$; $H_s < 0$, $H_L < 0$; and $H_s < 0$, $H_L > 0$ represent more than 90% of the observations. The $H_s < 0$, $H_L < 0$ combination was the most prevalent case; Fig. 3 shows this regime as all but the weakly stable region in the right panel.

The other two common cases—$H_s > 0$, $H_L > 0$ and $H_s < 0$, $H_L > 0$—typically occur 10–30% of the time over sea ice and are associated with weakly unstable or weakly stable stratification.

In creating flux algorithms for the SHEBA and Ice Station Weddell data, Andreas et al. (2005, 2010a, 2010b) had screened the H_s, H_L, $\Delta\Theta$, and ΔQ data and excluded small values that may have been below the uncertainty limits of the instruments. We have done no such screening here because it might bias the results. For example, H_s, H_L, $\Delta\Theta$, and ΔQ are likely all small in the $H_s < 0$, $H_L > 0$ regime (see Fig. 3). In other words, Table 1 is based on all available data.

5. Bo–Bo_* RELATIONS

Figures 4, 5, and 6 show Bo versus Bo_*—based on the SHEBA and Ice Station Weddell eddy-covariance measurements of H_s and H_L—for the three dominant flux combinations: $H_s > 0$, $H_L > 0$; $H_s < 0$, $H_L < 0$; and $H_s < 0$, $H_L > 0$, respectively. In each figure, the red line is the best fit through the data for which the power of Bo_* is one in these log-log plots.

Hence, for $H_s > 0$ and $H_L > 0$,

$$Bo = (0.76 \pm 0.09)Bo_* \; ; \qquad (5.1)$$

for $H_s <$ and $H_L < 0$,

$$Bo = (3.58 \pm 0.57)Bo_* \; ; \qquad (5.2)$$

and for $H_s < 0$ and $H_L > 0$,

$$Bo = -(1.35 \pm 0.31)Bo_* \; . \qquad (5.3)$$

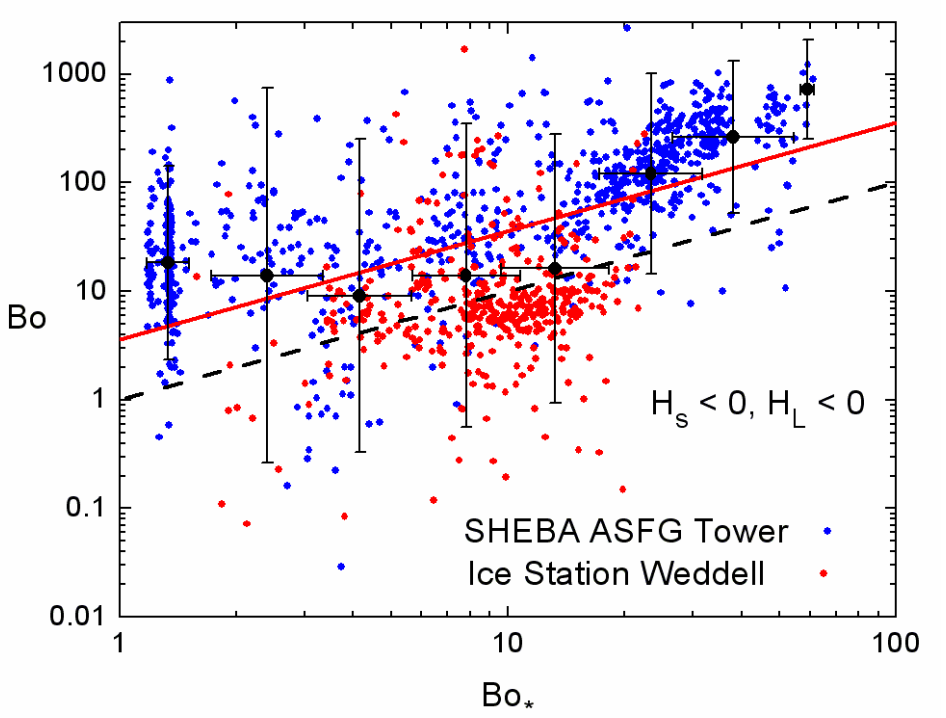

FIG. 5. As in Fig. 4, except this shows cases for which $H_s < 0$ and $H_L < 0$. The red line is (5.2).

The coefficients in these are somewhat different from Andreas and Cash's (1996) results, which include cases over water for which Bo_* was often less than one.

The results (5.1), (5.2), and (5.3) do, nevertheless, satisfy the constraints expressed in (2.5), (2.7), and (2.8), respectively. That is, on average, $Bo < Bo_*$ for the $H_s > 0$, $H_L > 0$ regime; $Bo > Bo_*$ for the $H_s < 0$, $H_L < 0$ regime; and $Bo \approx -Bo_*$ for the $H_s < 0$, $H_L > 0$ regime.

6. DISCUSSION AND CONCLUSIONS

As in Andreas and Cash's (1996) analysis, we likewise find that the sensible and latent heat fluxes over saturated surfaces—in this case, Arctic and Antarctic sea ice—occur predominantly in three combinations: $H_s > 0$, $H_L > 0$; $H_s < 0$, $H_L < 0$; and $H_s < 0$, $H_L > 0$. In our 28,000 hours of data, these three combinations represented 95% of the cases. In essence, these are the only three non-trivial combinations that can occur when the surface is saturated and the humidity above the surface is not super-saturated.

In each of these three flux regimes, the quantity Bo_*, (2.3), provides a theoretical constraint on the resulting Bowen ratio, Bo. Using eddy-covariance measurements of H_s and H_L from SHEBA and Ice Station Weddell, we confirmed those constraints in Figs. 4, 5, and 6 and in equations (5.1), (5.2), and (5.3).

The data in Figs. 4–6 are very scattered, however; and the coefficients in (5.1)–(5.3) are all close to one. We could therefore reasonably simplify (5.1)–(5.3) into the single result

$$|Bo| = Bo_* \qquad (6.1)$$

for all three flux regimes.

We envision several possible uses for these results. One is as a quality control on measurements or estimates of H_s and H_L. The obtained values should have a climatology similar to those in Table 1. The inferred Bowen ratio should also depend on surface temperature as predicted in (5.1)–(5.3).

In fact, (5.1)–(5.3) can supply an estimate of the Bowen ratio in any of the many applications that require it.

In particular, (5.1)–(5.3) provide relations between sensible and latent heat fluxes that could be key components for estimating the surface energy budget over sea ice from satellites. For example, Bentamy et al. (2003) demonstrated that satellite sensors can yield estimates of wind speed

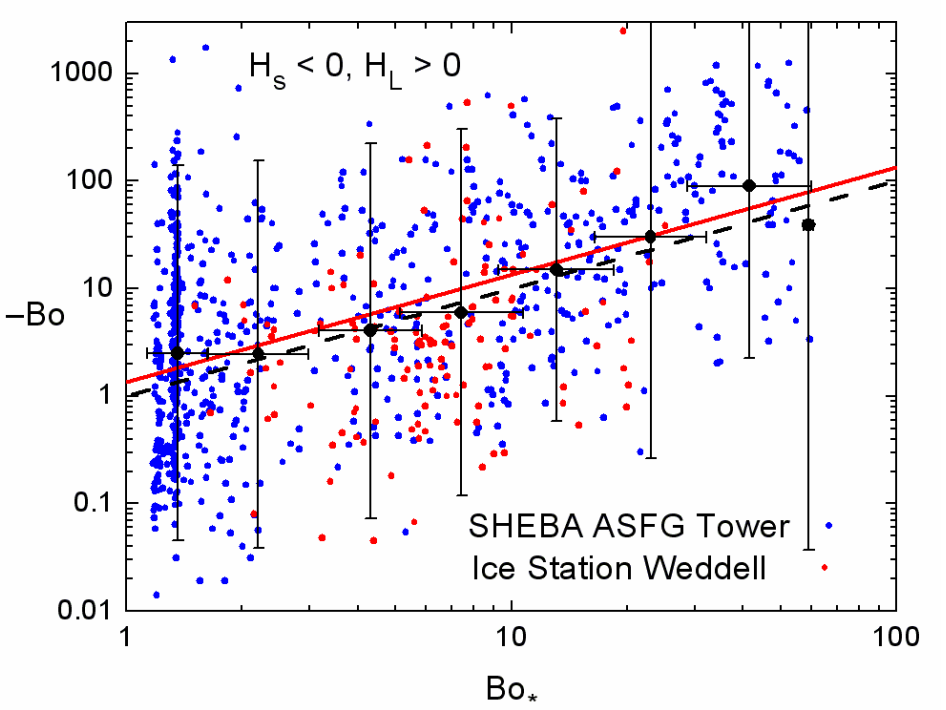

FIG. 6. As in Fig. 4, except this shows cases for which $H_s < 0$ and $H_L > 0$. Notice, the vertical axis represents –Bo. The red line is (5.3).

and $Q_s - Q_r$ over the open ocean; H_L follows immediately from (1.2b). And H_s could then easily come from relationships like (1.1) and (5.1)–(5.3) because surface temperature is a typical satellite measurement. Moreover, satellites can provide estimates of all the radiation components in the surface energy budget. Finally, the remaining term in the energy budget, the conductive flux to the surface up from the snow and ice, could be obtained with a simple heat conduction equation and satellite measurements of water and ice surface temperatures.

7. ACKNOWLEDGMENTS

We thank our colleagues in the SHEBA Atmospheric Surface Flux Group for helping us collect, process, and interpret the SHEBA data: Chris Fairall, Andrey Grachev, Peter Guest, Tom Horst, and Ola Persson. We also thank the other members of the meteorological team on Ice Station Weddell for their help: Kerry Claffey, Boris Ivanov, and Aleksandr Makshtas. The U.S. National Science Foundation supported this work with awards. OPP 06-11942 and OPP 10-19322. The National Science Foundation also supported our research on Ice Station Weddell and during SHEBA with previous awards.

8. REFERENCES

Andreas, E. L, 1988: Estimating C_n^2 over snow and sea ice from meteorological data. *J. Opt. Soc. Amer. A*, **5**, 481–495.

____, 1989: Comments on "A physical bound on the Bowen ratio." *J. Appl. Meteor.*, **28**, 1252–1254.

____, 1992: Uncertainty in a path-averaged measurement of the friction velocity u_*. *J. Appl. Meteor.*, **31**, 1312–1321.

____, and B. A. Cash, 1996: A new formulation for the Bowen ratio over saturated surfaces. *J. Appl. Meteor.*, **35**, 1281–1289.

____, P. S. Guest, P. O. G. Persson, C. W. Fairall, T. W. Horst, R. E. Moritz, and S. R. Semmer, 2002: Near-surface water vapor over polar sea ice is always near ice saturation. *J. Geophys. Res.*, **107** (C10), doi: 10.1029/2000JC000411.

____, R. E. Jordan, and A. P. Makshtas, 2004: Simulations of snow, ice, and near-surface atmospheric processes on Ice Station Weddell. *J. Hydrometeor.*, **5**, 611–624.

____, ____, and ____, 2005. Parameterizing turbulent exchange over sea ice: The Ice Station Weddell results. *Bound.-Layer*

Meteor., **114**, 439–460.

____, T. W. Horst, A. A. Grachev, P. O. G. Persson, C. W. Fairall, P. S. Guest, and R. E. Jordan, 2010a: Parameterising turbulent exchange over summer sea ice and the marginal ice zone. *Quart. J. Roy. Meteor. Soc.*, **136**, 927–943.

____, P. O. G. Persson, R. E. Jordan, T. W. Horst, P. S. Guest, A. A. Grachev, and C. W. Fairall, 2010b: Parameterizing turbulent exchange over sea ice in winter. *J. Hydrometeor.*, **11**, 87–104.

Arya, S. P., 1988: *Introduction to Micrometeorology*. Academic Press, 307 pp.

Bentamy, A., K. B. Katsaros, A. M. Mestas-Nuñez, W. M. Drennan, E. B. Forde, and H. Roquet, 2003: Satellite estimates of wind speed and latent heat flux over the global ocean. *J. Climate*, **16**, 637–656.

Brutsaert, W. H., 1982: *Evaporation into the Atmosphere: Theory, History, and Applications*. D. Reidel, 299 pp.

Busch, N. E., 1973: On the mechanics of turbulence. *Workshop on Micrometeorology*, D. A. Haugen, Ed., American Meteorological Society, 1–65.

Dyer, A. J., 1974: A review of flux-profile relationships. *Bound.-Layer Meteor.*, **7**, 363–372.

Fairall, C. W., E. F. Bradley, D. P. Rogers, J. B. Edson, and G. S. Young, 1996: Bulk parameterization of air-sea fluxes for Tropical Ocean-Global Atmosphere Coupled-Ocean Atmosphere Response Experiment. *J. Geophys. Res.*, **101** (C2), 3747–3764.

Fleagle, R. G., and J. A. Businger, 1980: *An Introduction to Atmospheric Physics, 2nd Ed*. Academic Press, 432 pp.

Garratt, J. R., 1992: *The Atmospheric Boundary Layer*. Cambridge University Press, 316 pp.

Hicks, B. B., and G. D. Hess, 1977: On the Bowen ratio and surface temperature at sea. *J. Phys. Oceanogr.*, **7**, 141–145.

Högström, U., 1996: Review of some basic characteristics of the atmospheric surface layer. *Bound.-Layer Meteor.*, **78**, 215–246.

Jo, Y.-H., X.-H. Yan, J. Pan, M.-X. He, and W. T. Liu, 2002: Calculation of the Bowen ratio in the tropical Pacific using sea surface temperature data. *J. Geophys. Res.*, **107** (C9), doi: 10.1029/2001JC001150.

Lewis, J. M., 1995: The story behind the Bowen ratio. *Bull. Amer. Meteor. Soc.*, **76**, 2433–2443.

Militzer, J. M., M. C. Michaelis, S. R. Semmer, K. S. Norris, T. W. Horst, S. P. Oncley, A. C. Delany, and F. V. Brock, 1995: Development of the prototype PAM III/Flux-PAM surface meteorological station. Preprints, *Ninth Symp. on Meteorological Observations and Instrumentation*, Charlotte, NC, American Meteorological Society, 490–494.

Panofsky, H. A. and J. A. Dutton, 1984: *Atmospheric Turbulence: Models and Methods for Engineering Applications*. John Wiley and Sons, 397 pp.

Persson, P. O. G., C. W. Fairall, E. L Andreas, P. S. Guest, and D. K. Perovich, 2002: Measurements near the Atmospheric Surface Flux Group tower at SHEBA: Near-surface conditions and surface energy budget. *J. Geophys. Res.*, **107** (C10), doi: 10.1029/2000JC000705.

Philip, J. R., 1987: A physical bound on the Bowen ratio. *J. Climate Appl. Meteor.*, **26**, 1043–1045.

____, 1989: Reply. *J. Appl. Meteor.*, **28**, 1255.

Priestley, C. H. B., and R. J. Taylor, 1972: On the assessment of surface heat flux and evaporation using large-scale parameters. *Mon. Wea. Rev.*, **100**, 81–92.

Raupach, M. R., 2001: Combination theory and equilibrium evaporation. *Quart. J. Roy. Meteor. Soc.*, **127**, 1149–1181.

Schotanus, P., F. T. M. Nieuwstadt, and H. A. R. De Bruin, 1983: Temperature measurement with a sonic anemometer and its application to heat and moisture fluxes. *Bound.-Layer Meteor.*, **26**, 81–93.

Stull, R. B., 1988: *An Introduction to Boundary Layer Meteorology*. Kluwer, 666 pp.

Wesley, M. L., 1976: The combined effect of temperature and humidity fluctuations on refractive index. *J. Appl. Meteor.*, **15**, 43–49.